Microtraps for atoms outside a fiber illuminated perpendicular to its axis: Numerical results

Fam Le Kien* and K. Hakuta
Department of Applied Physics and Chemistry, University of Electro-Communications, Chofu, Tokyo 182-8585, Japan
(Received 21 April 2009; published 24 July 2009)

We show theoretically that a vacuum-clad silica-core fiber can focus a perpendicularly incident light onto one or several lines parallel to the fiber axis. We demonstrate numerically that such a focusing action of the fiber can be used to trap and to guide atoms along the fiber with a red- or a blue-detuned incident light.

DOI: 10.1103/PhysRevA.80.013415 PACS number(s): 37.10.Gh, 37.10.Vz, 03.75.Be, 32.80.Qk

I. INTRODUCTION

Trapping and guiding neutral atoms are key problems of matter-wave physics [1,2]. Atom traps and atom waveguides can be used as tools for atom optics, atom interferometry, atom lithography, quantum information processing with neutral atoms, precision force sensing, and studies of the interaction between atoms and surfaces [3]. Atoms can be trapped and manipulated by the gradient dipole forces of light waves [1,4]. A focused Gaussian laser beam tuned far below the atomic resonance frequency represents the simplest dipole trap [1,4]. Evanescent light waves have also been used extensively to trap and to guide atoms since they have high spatial gradients and use rigid dielectric structures such as prisms and fibers to define the potential shape [5–7]. Of great interest is the ability of waveguides and microtraps to confine atoms, providing high optical densities, strong interactions with light, and mechanisms for transporting atoms. Cold atoms have been trapped and guided by far-detuned lights inside a hollow capillary fiber [8] or a hollow-core photonic crystal fiber [9].

A method for trapping and guiding neutral atoms outside a fiber has been proposed [6]. This method has been studied in the case of large-radius fibers [6] and in the case of nanofibers [10,11]. The method requires the use of a single (red-detuned) light beam [6,10] or two (red- and blue-detuned) light beams [6,11] launched into the fiber. In the single-color scheme [6,10], the trapping is achieved by the balance between the optical dipole force of a red-detuned light field and the centrifugal force on a spinning atom. In the two-color scheme [6,11], the trapping is achieved by the balance between the optical dipole forces of red-detuned and blue-detuned light fields. The optical dipole forces used in the above schemes are produced by the gradient of the field intensity in the radial direction. Such forces are conservative. When the fields are far from resonance with the atom, the dissipative forces are negligible. Another way to produce a trap above a planar waveguide [12] or outside a fiber [13] is to use interference between different transverse modes with the same color to obtain both attractive and repulsive forces.

In this paper, we show theoretically that a vacuum-clad silica-core fiber can focus a perpendicularly incident light onto one or several lines parallel to the fiber axis. We demonstrate numerically that the optical potential for the atoms may have one or several local minimum points in the transverse plane and, therefore, the atoms can be confined and guided along one or several straight lines parallel to the fiber axis.

The paper is organized as follows. In Sec. II we describe the ability of a vacuum-clad silica-core fiber to focus an incident light. In Sec. III we examine the optical potential of a cesium atom in a far-detuned fiber-focused light field. In Sec. IV we present the results of our numerical calculations. Our conclusions are given in Sec. V.

II. FOCUSING LIGHT BY A FIBER

Consider an optical fiber that has a cylindrical silica core of radius a and of refractive index n and an infinite vacuum clad of refractive index $n_0=1$. Such a fiber can be prepared using taper fiber technology. The essence of the technology is to heat and adiabatically pull a conventional optical fiber to a small thickness. Due to tapering, the original core is almost vanishing. Therefore, the refractive indices that determine the guiding properties of the tapered fiber are the refractive index of the original silica clad and the refractive index of the surrounding vacuum. The refractive index and the radius of the tapered silica clad will be henceforth referred to simply as the fiber refractive index n and the fiber radius a, respectively. We use the Cartesian coordinates $\{x,y,z\}$ and the cylindrical coordinates $\{r,\varphi,z\}$, where z is the fiber axis.

Let an atom be moving in a potential U outside the fiber. If U has a local minimum at a point outside the fiber, the atom can be trapped in the vicinity of this point. Our task is to create a potential with a trapping minimum sufficiently far from the fiber surface to make the effects of surface interaction and heating negligible. For this purpose, we shine a plane-wave laser light with frequency ω into the fiber. The laser field is incident along the transverse direction x, which is perpendicular to the fiber axis z. A schematic of our design is shown in Fig. 1.

Outside the fiber, the total field comprises of the incident field and the scattered one. Without loss of generality, we examine a particular case where the field is of TM polarization. In this case, the electric component of the total field is aligned along the fiber axis z. The amplitude of the total field outside the fiber is given by [14]

*Also at Institute of Physics, Vietnamese Academy of Science and Technology, Hanoi, Vietnam.

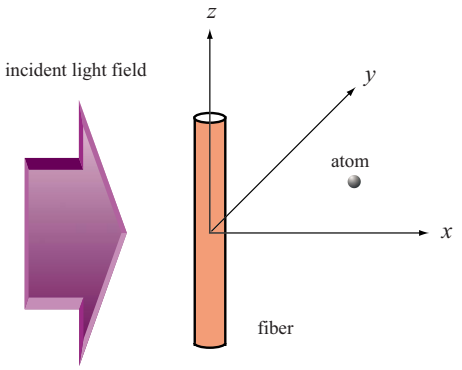

FIG. 1. (Color online) Schematic of atom trapping in the vicinity of an optical fiber illuminated perpendicular to its axis.

$$E = E_0\left(e^{ikr\cos\varphi} - \sum_{l=-\infty}^{\infty} i^l b_l H_l^{(1)}(kr)e^{il\varphi}\right), \tag{1}$$

where E_0 is the amplitude of the incident field, the expansion coefficients

$$b_l = \frac{nJ_l'(nka)J_l(ka) - J_l(nka)J_l'(ka)}{nJ_l'(nka)H_l^{(1)}(ka) - J_l(nka)H_l'^{(1)}(ka)} \tag{2}$$

characterize the scattered field, J_l are the Bessel functions of the first kind, and $H_l^{(1)}$ are the Hankel functions of the first kind. Here $k=2\pi/\lambda$ is the wave number, with λ being the wavelength of the incident wave.

We plot in Fig. 2 the spatial profiles of the intensity $|E|^2$

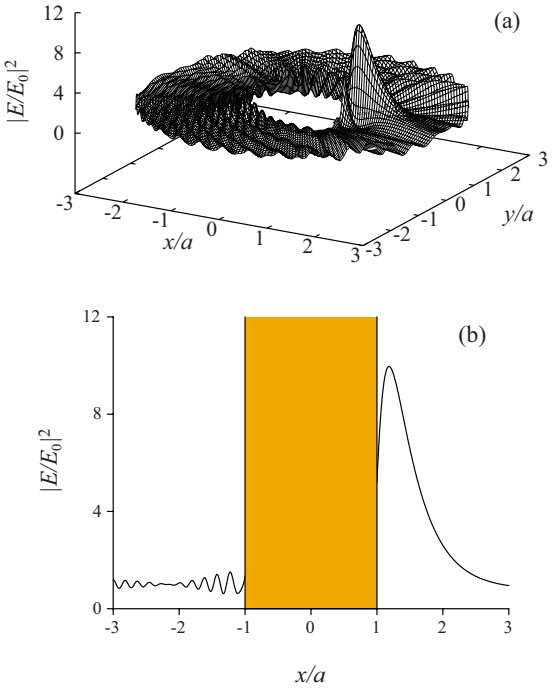

FIG. 2. (Color online) Spatial profiles of the intensity $|E|^2$ (a) over the exterior cross section of the fiber and (b) along the incidence direction x of the illumination beam. The field polarization is TM. The fiber radius is $a=2.5$ μm. The field wavelength is $\lambda=900$ nm.

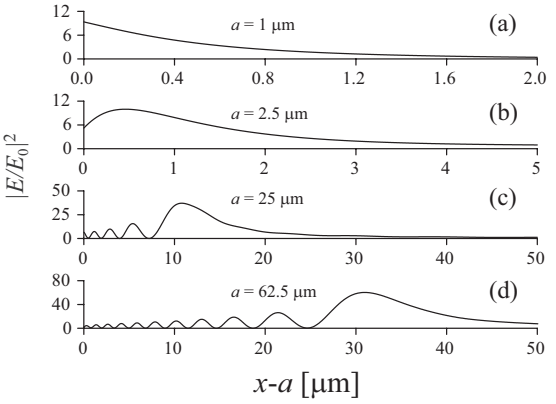

FIG. 3. Spatial profiles of the intensity $|E|^2$ along the x axis for various values of the fiber radius a. The incident wave propagates in the $+x$ direction. The field polarization is TM. The field wavelength is $\lambda=900$ nm.

over the exterior cross section of the fiber and along the incidence direction x of the illumination beam for the parameters $a=2.5$ μm and $\lambda=900$ nm. The figure shows that the intensity has a peak behind the fiber. The appearance of such a peak is a result of the focusing action of the fiber [14,15]. The focusing of light by a fiber has been investigated theoretically and demonstrated experimentally [15]. If the light field is red-detuned from a dominant atomic transition, the atom will seek for the strong field. In this case, the focus point in the fiber cross-section plane can act as a trapping point for the atom. Due to the axial symmetry, each trapping point in the cross-section plane corresponds to a trapping line in the three-dimensional space. Atoms trapped along such a line can be transported along and guided by the fiber.

We plot in Fig. 3 the spatial profiles of the intensity $|E|^2$ along the x axis for various values of the fiber radius a. The figure shows that, when the fiber radius a (or, equivalently, the size parameter ka) is large enough, the field intensity $|E|^2$ has one or several local peaks behind the fiber. For $n=1.45$, we find the condition $ka \geq \xi_0 \cong 9$ for a focus point to occur behind the fiber. When the fiber radius increases and does not correspond to morphology-dependent resonances, the normalized height $I_{\max}=|E_{\max}/E_0|^2$ of the main intensity peak increases and the normalized radial location $x_{\max}/a$ of this peak moves away from the surface until it reaches the geometrical optics limit ($x_{\max}/a$ increases to about 1.58 for $n=1.45$), in full agreement with the results of Ref. [15]. The peaks outside the fiber can be used to trap atoms if the light field is red-detuned from a dominant atomic transition. Meanwhile, the minimum points, which appear in the regions between two adjacent peaks, can be used to trap atoms when the light field is blue-detuned. Atoms trapped along intensity-peak lines in the case of red detunings or intensity-minimum lines in the case of blue detunings can be transported along and guided by the fiber.

We note that, for small size parameters, namely, for $ka < \xi_0 \cong 9$, the intensity of the field behind the fiber is maximal at the surface and monotonically reduces with increasing distance [15]. Therefore, only fibers with large size parameters can focus perpendicularly incident light to produce optical dipole traps for atoms. When the size parameter ka is large,

the large-argument approximation can be used to simplify the calculations for the Bessel functions $J_l(ka)$ and $J_l(nka)$ and the Hankel functions $H_l^{(1)}(ka)$, which make up Eq. (2) for the scattering coefficients b_l. The condition for this approximation is $ka \gg l$. Meanwhile, the Bessel expansion (1) for the field outside the fiber contains the terms associated with all the integer orders l. In the vicinity of the focusing point $x_{\max} > a$, the terms associated with the orders $l \sim kx_{\max} > ka$ are significant. The large-argument approximation cannot be applied to such terms. Hence, the rigorous treatment for the field in the vicinity of the focusing point outside the fiber requires the computations of Eqs. (1) and (2). The dependences of the focused intensity and the focusing point location on the size parameter and the refractive index have been investigated in detail in Ref. [15].

III. POTENTIAL OF AN ATOM IN A FAR-OFF-RESONANCE FIELD

In this section, we describe the potential of an atom outside a fiber illuminated perpendicular to its axis. We assume that the atom is in the ground state and the applied field is far off resonance with the atom. Under the far-off-resonance condition, the atom spends most of its time in its ground state and, therefore, spontaneous scattering of light by the atom is weak. In this case, the radiation pressure force is small [4,16]. The dipole force can be derived from the optical potential [4,16,17]

$$U_{\text{opt}} = -\tfrac{1}{4}\alpha |E|^2, \tag{3}$$

where $\alpha = \alpha(\omega)$ is the real part of the atomic polarizability at the optical frequency ω. The factor 1/4 in Eq. (3) results from the fact that the dipole of the atom is not a permanent dipole but is induced by the field, giving 1/2, and from the fact that the intensity is averaged over optical oscillations, giving another 1/2.

Before we proceed, we briefly discuss the case of a two-level atom. In this case, the real part of the polarizability can be approximated as $\alpha = -\pi\epsilon_0 c^3 \gamma_0 / \omega_0^3 \Delta = -d^2/\hbar\Delta$. Here ω_0 and γ_0 are the frequency and the linewidth of the atomic transition, respectively; $\Delta = \omega - \omega_0$ is the detuning of the optical frequency ω from the atomic frequency ω_0; and d is the projection of the dipole moment onto the direction of the field polarization vector. In deriving the above approximation for α, it has been assumed that Δ is large as compared to the linewidth γ_0 but small as compared to the optical and the atomic frequencies ω and ω_0, respectively. The corresponding approximate expression for the optical potential of the atom is $U_{\text{opt}} = \hbar\Omega^2/\Delta$, where $\Omega = d|E|/2\hbar$ is the Rabi frequency. The sign of the optical potential is controlled by the sign of the field detuning Δ. When the detuning is red ($\Delta < 0$) or blue ($\Delta > 0$), the potential is attractive or repulsive, respectively. Such a potential may possess a local minimum point, leading to a possibility of atom trapping. Since U_{opt} is independent of z, a minimum point in the two-dimensional space $\{r, \varphi\}$ corresponds to a line of minimum points in the three-dimensional space $\{r, \varphi, z\}$.

We now consider a multilevel cesium atom. When the field frequency ω is far from resonance with the atomic frequencies, we must take into account the multilevel structure of the atom. The real part of the dynamical polarizability of the ground-state atom is given by

$$\alpha = \frac{1}{3\hbar}\sum_e \langle e\|D\|g\rangle^2 \frac{\omega_{eg}(\omega_{eg}^2 - \omega^2 + \gamma_e^2/4)}{(\omega_{eg}^2 - \omega^2 + \gamma_e^2/4)^2 + \gamma_e^2\omega^2}. \tag{4}$$

Here $\langle e\|D\|g\rangle$ is the reduced electric dipole matrix element for the transition between an excited fine-structure state $|e\rangle$ and the ground fine-structure state $|g\rangle$, $\omega_{eg} = \omega_e - \omega_g$ is the transition frequency, and γ_e is the population decay rate. The real part of the dynamical polarizability for atomic cesium has been calculated for a wide range of the optical frequency ω [18].

An atom near the surface of a medium experiences a van der Waals force. The van der Waals potential of an atom near the surface of a cylindrical dielectric rod is given by [19]

$$V(r) = \frac{\hbar}{4\pi^3\epsilon_0}\sum_{l=-\infty}^{\infty}\int_0^\infty dk[k^2 K_l'^2(kr) + (k^2 + l^2/r^2)K_l^2(kr)]\int_0^\infty d\xi\, \alpha(i\xi)G_l(i\xi), \tag{5}$$

where

$$G_l(i\xi) = \frac{[\epsilon(i\xi) - \epsilon_0]I_l(ka)I_l'(ka)}{\epsilon_0 I_l(ka)K_l'(ka) - \epsilon(i\xi)I_l'(ka)K_l(ka)}. \tag{6}$$

Here $\epsilon(\omega) = \epsilon_0 n^2(\omega)$ is the dynamical dielectric function and I_l and K_l are the modified Bessel functions of the first and the second kinds, respectively.

The total potential U of the atom is the sum of the optical potential U_{opt} and the van der Waals potential V, i.e.,

$$U = U_{\text{opt}} + V. \tag{7}$$

Equations (3), (5), and (7) allow us to calculate the total potential U.

In general, the polarizability of an atom is a complex characteristic. The imaginary part of the complex polarizability is given by [17]

$$\kappa = \frac{1}{3\hbar}\sum_e \langle e\|D\|g\rangle^2 \frac{\omega_{eg}\gamma_e\omega}{(\omega_{eg}^2 - \omega^2 + \gamma_e^2/4)^2 + \gamma_e^2\omega^2}. \tag{8}$$

This part is responsible for spontaneous scattering. The rate of spontaneous scattering caused by a light field E is given by $\Gamma_{\text{sc}} = \kappa|E|^2/4\hbar$. Spontaneous scattering limits the coherence time of the trap. The characteristic coherence time is $\tau_{\text{coh}} = \Gamma_{\text{sc}}^{-1}$ [20,21]. Every scattered photon imparts a recoil energy $\theta_{\text{rec}} = (\hbar k)^2/2M$ to the atom, where M is the mass of the atom. Therefore, the absorption of trapping field photons and the emission of other photons result in a loss of atoms from the trapping potential. For a trap depth U_D, the quantity $\tau_{\text{trap}} = U_D/(2\theta_{\text{rec}}\Gamma_{\text{sc}})$ characterizes the trap lifetime due to recoil heating [21]. When the light field frequency is near to an atomic resonance, the scattering rate is large and, therefore, the coherence time and the trap lifetime are small. In order to produce an optical dipole trap with a large coherence time, a large trap lifetime, and a small radiation pressure force, we must use a far-off-resonance field.

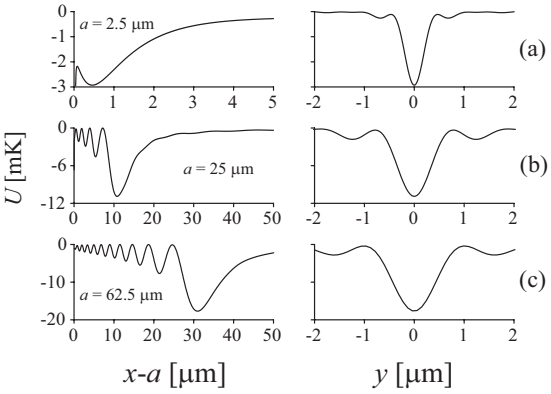

FIG. 4. Spatial profiles of the total potential U along the x direction (left column) and along the line passing in the y direction through the principal minimum point x_m (right column). The fiber radii are (a) 2.5, (b) 25, and (c) 62.5 μm. The intensity of the incident field is $I=10$ kW/cm^2. The field wavelength is $\lambda=900$ nm. The field polarization is TM. The incident wave propagates in the $+x$ direction.

IV. NUMERICAL RESULTS

In this section, we calculate numerically the total potential U of a ground-state cesium atom in an optical field focused by a fiber. The ground-state cesium atom has two strong transitions: at 894 nm (D_1 line) and 852 nm (D_2 line). We use a red-detuned or a blue-detuned field to create an attractive or a repulsive optical potential, respectively.

First, we explore the potential produced by an incident red-detuned light field. The wavelength of the incident light is assumed to be $\lambda=900$ nm. The detunings of the laser field from the dominant D_1 and D_2 lines of the cesium atom are $\Delta_1=-2.1$ THz and $\Delta_2=-18.7$ THz, respectively. The input intensity of the incident light is assumed to be 10 kW/cm^2. Such an intensity is high as compared to the resonance saturation intensity (1.1 mW/cm^2 for the cesium D_2 line [16]). However, the Rabi frequency of such an incident field is on the order of 10 GHz, which is still very small as compared to the detunings of the field from the dominant lines. We plot in Fig. 4 the spatial profiles of the total potential U along the x direction (left column) and along the line passing in the y direction through the principal minimum point x_m (right column). The fiber radii are 2.5 μm [Fig. 4(a)], 25 μm [Fig. 4(b)], and 62.5 μm [Fig. 4(c)]. Such values of the fiber radius are large enough to produce one or several potential minima behind the fiber.

Note that the waists of the illumination beams need to be at least 10, 100, and 250 μm in the cases of Figs. 4(a)–4(c), respectively. The illumination beam intensity of 10 kW/cm^2, used for the calculations, can be obtained by focusing a laser beam with a power on the order of 10 mW to a waist of 10 μm. Such a beam waist size is acceptable for the case of Fig. 4(a), where the fiber diameter is $2a=5$ μm. In the cases of Figs. 4(b) and 4(c), where the fiber diameters are $2a=50$ and 125 μm, respectively, powers on the order of 1 and 6.25 W, respectively, are required to achieve the intensity of 10 kW/cm^2 for the illumination beams with waist sizes on the order of 100 and 250 μm, respectively. Such powers are rather high. However, the larger fibers can focus the light more strongly (see Fig. 3 and Ref. [15]) and consequently can produce deeper potentials (see Fig. 4). Therefore, the above-estimated incident powers can be reduced. In order to show the effect of the fiber radius on the trap characteristics, we use the same illumination beam intensity for the figures.

We observe in Fig. 4(a) that the total potential has a local minimum $U_m\cong-2.93$ mK at the distance $x_m-a\cong0.46$ μm from the surface. The minimum point x_m in the axis x corresponds to the trapping point $(x=x_m,y=0)$ in the cross-section plane and to the line of trapping points $(x=x_m,y=0,z)$ in the three-dimensional space. The trap depth is $U_D\cong0.75$ mK. It is clear that the trapping point x_m is well outside the fiber. The van der Waals potential is only about -0.6 μK at the potential minimum point x_m and makes just a small contribution in the vicinity of x_m. We observe that the trap depth for the y direction is larger than that for the x direction. We find that the rate of scattering due to the trapping field at the potential minimum is $\Gamma^{(\mathrm{sc})}\cong348$ s^{-1}. The corresponding coherence time is $\tau_{\mathrm{coh}}\cong3$ ms. Since the recoil energy due to a single trapping-light photon is $\theta^{(\mathrm{rec})}\cong0.09$ μK, the trap lifetime due to recoil heating is estimated to be $\tau_{\mathrm{trap}}\cong12$ s. At the trapping point, the oscillation frequencies for the x and the y directions are $\omega_x\cong113$ kHz$\cong5.4$ μK and $\omega_y\cong367$ kHz$\cong18$ μK, respectively. The sizes of the ground states of the one-dimensional potentials for the vibrational motion along the x and the y directions are around 18.3 and 10.2 nm, respectively. The spatial extensions of the trap volume for cesium atoms with a kinetic energy of 100 μK are about 319 and 98 nm in the x and the y directions, respectively.

Figures 4(b) and 4(c) show that, when the fiber radius is large enough, several minimum points of the potential in the fiber cross-section plane $\{x,y\}$, which correspond to minimum lines of the potential in the three-dimensional space $\{x,y,z\}$, may occur. Each minimum line can, in principle, be used to trap atoms. In the cases of Figs. 4(b) and 4(c), the deepest (principal) local minima occur at the distances $x_m-a\cong11$ and 31 μm, respectively, and their depths are $U_D\cong11$ and 18 mK, respectively. Comparison among Figs. 4(a)–4(c) shows that an increase in the fiber radius leads to an increase in the number of potential minima and also to an increase in their depths. The increase in the number of minima is a result of the increase in the interference between the incident and the scattered lights. The increase in the potential depth is a result of the increase in the ability of the fiber to collect and focus light (see Fig. 3 and Ref. [15]). Comparison among Figs. 4(a)–4(c) also shows that an increase in the fiber radius leads to an increase in the distance from the principal potential minimum to the fiber surface and to an increase in the width of the minimum. Therefore, in order to produce narrow microtraps, the fiber radius must not be too large.

In the case of Fig. 4(b), we find that the rate of scattering at the principal potential minimum is $\Gamma^{(\mathrm{sc})}\cong1294$ s^{-1}, the coherence time is $\tau_{\mathrm{coh}}\cong0.8$ ms, and the trap lifetime is $\tau_{\mathrm{trap}}\cong48$ s. The oscillation frequencies for the x and the y directions are $\omega_x\cong55$ kHz$\cong2.6$ μK and $\omega_y\cong402$ kHz $\cong19$ μK, respectively, and the spatial extensions of the

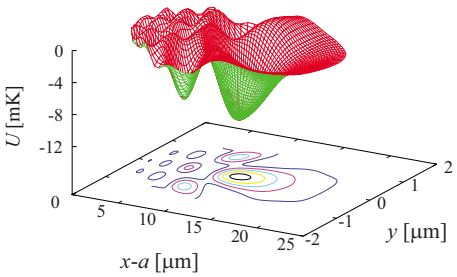

FIG. 5. (Color online) Spatial profile of the total potential U over part of the exterior cross section behind the fiber. The parameters used are as in Fig. 4(b).

ground states of the one-dimensional potentials along the x and the y directions are around 26.3 and 9.7 nm, respectively. The spatial extensions of the trap volume for cesium atoms with a kinetic energy of 100 μK are about 655 and 89 nm in the x and the y directions, respectively.

Similarly, in the case of Fig. 4(c), we find that the rate of scattering at the principal potential minimum is $\Gamma^{(sc)} \cong 2104$ s^{-1}, the coherence time is $\tau_{coh} \cong 0.5$ ms, and the trap lifetime is $\tau_{trap} \cong 48$ s. The oscillation frequencies for the x and the y directions are $\omega_x \cong 43$ kHz$\cong 2$ μK and $\omega_y \cong 402$ kHz$\cong 19$ μK, respectively, and the spatial extensions of the ground states of the one-dimensional potentials along the x and the y directions are around 29.9 and 9.7 nm, respectively. The spatial extensions of the trap volume for cesium atoms with a kinetic energy of 100 μK are about 840 and 89 nm in the x and the y directions, respectively.

Comparison among Figs. 4(a)–4(c) shows that the dependence of the size of the ground state in the y direction on the fiber radius is weak as compared to that in the x direction. Figures 4(b) and 4(c) show that the secondary minima are spatially narrower than the principal minimum. In addition to the minima that lie on the axis x, the potential U may have several minima off the axis. To illustrate the existence of such off-axis minima, we plot in Fig. 5 the spatial profile of U over part of the exterior cross section for the parameters of Fig. 4(b). We observe from the figure that there is a set of off-axis minima of the potential behind the fiber. Although they are shallower than the principal minimum, their depths are on the order of a few millikevins (for the parameters used). Such minima can also be used to trap atoms.

We now examine the potential produced by an incident blue-detuned light. For this purpose, we choose the wavelength $\lambda = 800$ nm. The detunings of the laser field from the dominant D_1 and D_2 lines of the atom are $\Delta_1 = 39.5$ THz and $\Delta_2 = 22.9$ THz, respectively. The input intensity of the incident light is again assumed to be 10 kW/cm^2. The fiber radius is chosen to be 25 μm. We plot in Fig. 6 the spatial profile of the total potential U along the incidence direction x of the illumination beam. The figure shows that the spatial profile of the potential in the x direction has several minima. We plot in Fig. 7 the spatial profiles of the total potential over part of the exterior cross section behind the fiber and in the vicinity of a minimum point, namely, the second deepest minimum point, which is marked by an arrow in Fig. 6 and is at the distance $x_m - a = 4.4$ μm from the surface. We find that the depth of the trap around this minimum point is 0.17 mK

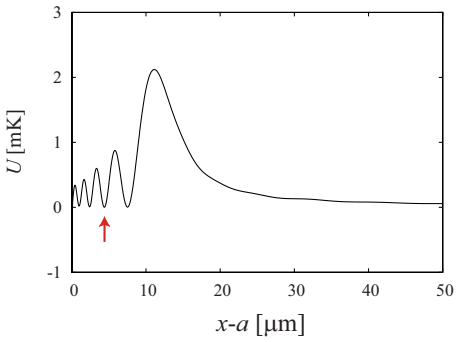

FIG. 6. (Color online) Spatial profile of the total potential U along the incidence direction x of the illumination beam. The field wavelength is $\lambda = 800$ nm. The fiber radius is 25 μm. The intensity of the incident field is $I = 10$ kW/cm^2. The field polarization is TM. The arrow marks the position of the second deepest minimum point, which is chosen for the plot in Fig. 7(b).

[see Fig. 7(b)], rather small as compared to the case of red detunings. However, the field intensity at the trapping point is small, and so is the scattering rate $\Gamma^{(sc)}$. Therefore, the coherence time τ_{coh} and the trap lifetime τ_{trap} are large. Indeed, we have $\Gamma^{(sc)} \cong 0.012$ s^{-1}, $\tau_{coh} \cong 80$ s, and $\tau_{trap} \cong 6 \times 10^4$ s at the trapping point. For cesium atoms with an initial kinetic energy of 100 μK, we have $\Gamma^{(sc)} \cong 1.4$ s^{-1}, $\tau_{coh} \cong 0.7$ s, and $\tau_{trap} \cong 220$ s. Note that we have used the modified formula $\tau_{trap} = (U_D - K)/(2\theta_{rec}\Gamma_{sc})$ to estimate the trap lifetime for atoms with a finite kinetic energy K. The oscillation frequencies for the x and the y directions are $\omega_x \cong 62$ kHz$\cong 3$ μK and $\omega_y \cong 36$ kHz$\cong 1.7$ μK, respectively, and the spatial extensions of the ground states of the one-dimensional potentials along the x and the y directions are around 24.8 and 32.4 nm, respectively. The spatial extensions of the trap volume in the x and the y directions for cesium atoms with a kinetic energy of 100 μK are about 0.6 and 0.4 μm, respectively.

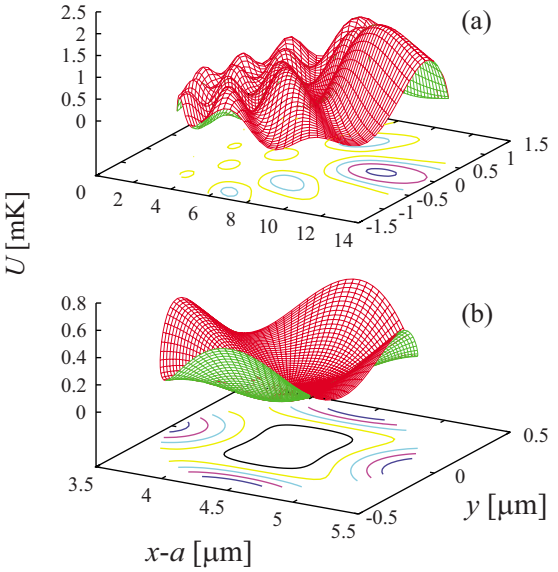

FIG. 7. (Color online) (a) Spatial profile of the total potential U over part of the exterior cross section behind the fiber. (b) Spatial profile of the total potential U in the vicinity of the minimum point marked by an arrow in Fig. 6. The parameters used are as in Fig. 6.

V. CONCLUSIONS

We have shown theoretically that an optical fiber can focus a perpendicularly incident light onto one or several lines parallel to the fiber axis. We have demonstrated numerically that the focusing action of the fiber can be used to trap and to guide atoms along the fiber with a red- or a blue-detuned incident light. We note that loading atoms into such a fiber-based dipole trap can be realized using conventional techniques such as optical molasses or magneto-optical traps to cool atoms [4]. Unlike conventional optical lenses, the fiber can create traps along several lines and can work not only with red-detuned light but also with blue-detuned light. Using such a scheme, it is possible to produce one-dimensional atomic samples (atomic lines or atomic arrays). The alignment of the fiber along another structure, such as a nanofiber [22] or a toroidal microresonator [23], may provide an efficient coupling of trapped atoms to the structure. In addition, it is possible to study the effects of surface-atom interaction on the propagation of light in a spatially extended atomic medium.

ACKNOWLEDGMENT

We thank K. Nayak for fruitful discussions.

[1] A. Ashkin, Phys. Rev. Lett. **24**, 156 (1970); **40**, 729 (1978); J. P. Gordon and A. Ashkin, Phys. Rev. A **21**, 1606 (1980); A. Ashkin, Science **210**, 1081 (1980); Opt. Lett. **9**, 454 (1984); Proc. Natl. Acad. Sci. U.S.A. **94**, 4853 (1997).

[2] S. Chu, Rev. Mod. Phys. **70**, 685 (1998); C. Cohen-Tannoudji, *ibid.* **70**, 707 (1998); W. D. Phillips, *ibid.* **70**, 721 (1998).

[3] C. S. Adams, M. Sigel, and J. Mlynek, Phys. Rep. **240**, 143 (1994); V. I. Balykin and V. S. Letokhov, *Atom Optics with Laser Light*, Laser Science and Technology Vol. 18 (Harwood Academic, New York, 1995), p. 115; P. Meystre, *Atom Optics* (Springer, New York, 2001), p. 311; J. Fortágh and C. Zimmermann, Rev. Mod. Phys. **79**, 235 (2007).

[4] A. P. Kazantsev, G. J. Surdutovich, and V. P. Yakovlev, *Mechanical Action of Light on Atoms* (World Scientific, Singapore, 1990); R. Grimm, M. Weidemüller, and Yu. B. Ovchinnikov, Adv. At., Mol., Opt. Phys. **42**, 95 (2000); V. I. Balykin, V. G. Minogin, and V. S. Letokhov, Rep. Prog. Phys. **63**, 1429 (2000).

[5] R. J. Cook and R. K. Hill, Opt. Commun. **43**, 258 (1982); V. I. Balykin, V. S. Letokhov, Yu. B. Ovchinnikov, and A. I. Sidorov, Phys. Rev. Lett. **60**, 2137 (1988).

[6] J. P. Dowling and J. Gea-Banacloche, Adv. At., Mol., Opt. Phys. **37**, 1 (1996).

[7] V. I. Balykin, Adv. At., Mol., Opt. Phys. **41**, 181 (1999).

[8] M. A. Ol'Shanii, Yu. B. Ovchinnikov, and V. S. Letokhov, Opt. Commun. **98**, 77 (1993); M. J. Renn, D. Montgomery, O. Vdovin, D. Z. Anderson, C. E. Wieman, and E. A. Cornell, Phys. Rev. Lett. **75**, 3253 (1995); H. Ito, T. Nakata, K. Sakaki, M. Ohtsu, K. I. Lee, and W. Jhe, *ibid.* **76**, 4500 (1996); R. G. Dall, M. D. Hoogerland, K. G. H. Baldwin, and S. J. Buckman, J. Opt. B: Quantum Semiclassical Opt. **1**, 396 (1999); D. Müller, E. A. Cornell, D. Z. Anderson, and E. R. I. Abraham, Phys. Rev. A **61**, 033411 (2000).

[9] T. Takekoshi and R. J. Knize, Phys. Rev. Lett. **98**, 210404 (2007); C. A. Christensen, S. Will, M. Saba, G.-B. Jo, Y.-I. Shin, W. Ketterle, and D. Pritchard, Phys. Rev. A **78**, 033429 (2008).

[10] V. I. Balykin, K. Hakuta, Fam Le Kien, J. Q. Liang, and M. Morinaga, Phys. Rev. A **70**, 011401(R) (2004).

[11] Fam Le Kien, V. I. Balykin, and K. Hakuta, Phys. Rev. A **70**, 063403 (2004).

[12] K. Christandl, G. P. Lafyatis, S.-C. Lee, and J.-F. Lee, Phys. Rev. A **70**, 032302 (2004).

[13] G. Sagué, A. Baade, and A. Rauschenbeutel, New J. Phys. **10**, 113008 (2008).

[14] H. C. van de Hulst, *Light Scattering by Small Particles* (Dover, New York, 1981); P. W. Barber and S. C. Hill, *Light Scattering by Particles: Computational Methods* (World Scientific, Singapore, 1990).

[15] D. S. Benincasa, P. W. Barber, J.-Z. Zhang, W.-F. Hsieh, and R. K. Chang, Appl. Opt. **26**, 1348 (1987).

[16] H. J. Metcalf and P. van der Straten, *Laser Cooling and Trapping* (Springer, New York, 1999).

[17] J. D. Jackson, *Classical Electrodynamics*, 3rd ed. (Wiley, New York, 1999).

[18] Fam Le Kien, V. I. Balykin, and K. Hakuta, J. Phys. Soc. Jpn. **74**, 910 (2005).

[19] M. Boustimi, J. Baudon, P. Candori, and J. Robert, Phys. Rev. B **65**, 155402 (2002); M. Boustimi, J. Baudon, and J. Robert, *ibid.* **67**, 045407 (2003).

[20] A. H. Barnett, S. P. Smith, M. Olshanii, K. S. Johnson, A. W. Adams, and M. Prentiss, Phys. Rev. A **61**, 023608 (2000).

[21] J. P. Burke, Jr., Sai-Tak Chu, G. W. Bryant, C. J. Williams, and P. S. Julienne, Phys. Rev. A **65**, 043411 (2002).

[22] L. Tong, R. R. Gattass, J. B. Ashcom, S. He, J. Lou, M. Shen, I. Maxwell, and E. Mazur, Nature (London) **426**, 816 (2003); T. A. Birks, W. J. Wadsworth, and P. St. J. Russell, Opt. Lett. **25**, 1415 (2000); K. P. Nayak, P. N. Melentiev, M. Morinaga, Fam Le Kien, V. I. Balykin, and K. Hakuta, Opt. Express **15**, 5431 (2007); G. Sagué, E. Vetsch, W. Alt, D. Meschede, and A. Rauschenbeutel, Phys. Rev. Lett. **99**, 163602 (2007).

[23] D. K. Armani, T. J. Kippenberg, S. M. Spillane, and K. J. Vahala, Nature (London) **421**, 925 (2003); S. M. Spillane, T. J. Kippenberg, K. J. Vahala, K. W. Goh, E. Wilcut, and H. J. Kimble, Phys. Rev. A **71**, 013817 (2005); T. Aoki, A. S. Parkins, D. J. Alton, C. A. Regal, B. Dayan, E. Ostby, K. J. Vahala, and H. J. Kimble, Phys. Rev. Lett. **102**, 083601 (2009).